Aeroengine Robust Gain-Scheduling Control Based on Performance Degradation

LINFENG GOU, ZHIDAN LIU[ID], DING FAN, AND HUA ZHENG[ID]

School of Power and Energy, Northwestern Polytechnical University, Xi'an 710119, China

Corresponding author: Zhidan Liu (liuzhidan@mail.nwpu.edu.cn)

ABSTRACT This study was conducted to develop a novel tracking control strategy for aeroengines with strong nonlinearity and uncertainty. Compared to existing robust gain-scheduling control strategies, the proposed control strategy has relatively low conservatism and can markedly improve engine performance. An improved on-board adaptive aeroengine model was established to estimate engine performance degradation and eliminate the degradation term contained in the perturbation block of the engine uncertain model in the design process. Robust controllers under engine normal and performance degradation states were designed at a set of operating points and scheduled according to relevant scheduling and health parameters. A desired robust gain-scheduling controller, which works based on performance degradation, can be precisely constructed via this approach. Simulation results are given to demonstrate the effectiveness of the proposed method, where the response speed of engine is improved by 38%.

INDEX TERMS Robust conservative, performance degradation, aeroengine, gain-scheduling, nonlinear system.

I. INTRODUCTION

The modern aeroengine is a complex nonlinear dynamic system with a wide range of functions and parameters. Its working state changes continuously with changes in external conditions and flight conditions. Any engine model as-established based on the aerodynamic thermodynamic relationship of its components is a strong nonlinear model [1], [2].

Many previous researchers have explored nonlinear systems [3]–[9]. Zhao *et al.* [3], for example, proposed a fuzzy-approximation-based asymptotic tracking control for a class of uncertain switched nonlinear systems. Most fuzzy adaptive control strategies can only achieve bounded error tracking performance, but this control scheme can guarantee local asymptotic tracking performance for the uncertain switched nonlinear system under consideration. Wang *et al.* [4] proposed an adaptive neural output-feedback decentralized control scheme for large-scale nonlinear systems with stochastic disturbances which guarantees that all signals in the closed-loop system are semi-globally uniformly ultimately bounded in the fourth-moment. Wang *et al.* [5] researched the adaptive fuzzy finite-time control of nonlinear systems with actuator faults. Wang *et al.* [6] built a fault-tolerant tracking control strategy for Takagi Sugeno fuzzy model-based nonlinear systems which combines integral sliding mode control and

adaptive control techniques. Li *et al.* [8] explored adaptive fuzzy tracking control for a class of uncertain switched nonlinear systems considering arbitrary switching, unmodeled dynamics, input saturation, unknown dead-zone output, dynamic disturbances, and unmeasurable states, which makes their results widely applicable.

Existing control methods for strong nonlinear systems tend to be inconvenient. For example, the feedback linearization method requires a high-precision nonlinear model [10]; the sliding mode control has chattering problems [11] and fuzzy control relies on prior knowledge [12]. Linear methods can be applied in the gain-scheduling context to control nonlinear or time-varying systems [13], [14]. The control performance of these systems is very prominent, so gain-scheduling control can be used to process various nonlinear problems [15]–[19]. As a typical strong nonlinear system, gain-scheduling control can be widely applied in the control of aircraft engines [20]–[27].

Jung *et al.* [21] and Yazar *et al.* [25] designed linear controllers using the proportion-integra-derivative (PID) technique, where PID controllers are linked via gain-scheduling to a tail-sitter unmanned aerial vehicles and a small-scale turbojet aeroengine, respectively. The limits of the PID controller can be mitigated by the so-called L_1 adaptive controller, which considers the coupling effect [21]. Yasar *et al.* [22] designed a gain-scheduling feedback controller for a turbofan engine to maintain specified performance. In an effort to resolve the problem

---

of speed-control at startup, Rodriguez-Martinez *et al.* [23] designed a PI fuzzy gain-scheduling controller for a gas-turbine power plant by synthesizing a gain-scheduling controller from multiple locally tuned generalized proportional integral algorithms in a fuzzy system; theirs outperformed the traditional single PI controller. Gilbert *et al.* [24] systematically designed gain-scheduling control laws with low complexity for a turbofan engine by extending another polynomial fixed-order controller design to SISO gain-scheduling with guaranteed stability and H_∞ performance over the whole scheduling parameter range. Pakmehr *et al.* [27] demonstrated the stability of gain-scheduling control for gas turbine engines.

Due to the undue influence of modeling errors, artificial model reduction for convenience, engine degradation over long-term operation, external interference, noise, and other factors, a controller designed for the nominal model may not give the actual system stability or enhanced performance even when it can effectively control the nominal model. Many previous researchers have explored robust gain-scheduling control as an alternative [28]–[33]. Peng *et al.* [28] used a series of decoupling controllers to formulate a multivariable gain-scheduled controller which has strong decoupling performance and robustness in large-transient turbofan engines. Wolodkin *et al.* [29] designed H_∞ controllers at fixed operating points for linear parameter variable (LPV) systems of a turbofan engine. Their gain-scheduled controller was obtained directly as part of the described design process, as opposed to conventional processes wherein it would be established after-the-fact to connect point designs. The National Aeronautics and Space Administration (NASA) Glenn Research Center (GRC) developed a unified robust multivariable approach which encompasses a series of H_∞ controllers and a simplified controller scheduling scheme for propulsion control.

The above robust gain-scheduling control techniques have strong robustness for aeroengines. However, they are very conservative as they consider engine degradation as an uncertainty. In fact, the degree of engine performance degradation can be estimated by measuring certain parameters [34]–[40]. In the late 1980s, Luppold *et al.* [34] first combined the engine on-board model with a Kalman filter to establish an on-board adaptive aeroengine model for estimating engine performance degradation. However, as the engine degrades, the steady-state reference value of the nonlinear model appears to be biased resulting in estimation errors. Xue Wei and Guo Yingqing [35] estimated the health condition of an engine over its lifetime by tracking filters. They applied a bank of Kalman filters for fault detection and isolation (FDI) sensors in the engine. Liu *et al.* [36] updated the health reference baseline for an airborne engine model via channel controller to accurately estimate engine degradation. Liu *et al.* [39] established a new adaptive modeling method with an equilibrium manifold for aeroengines that is accurate and simple in structure.

The above estimations of engine performance degradation can be used in engine fault diagnosis to maintain effectiveness as the engine degrades, but are not used for robust gain-scheduling control. In actuality, the performance degradation of engine components can be assessed by establishing an on-board adaptive model. This allows degradation terms to be estimated in the uncertainty model, narrowing the scope of the uncertainty model and reducing the conservativeness of the robust gain-scheduled controller.

In this study, perturbation was added to the nominal model and a set of uncertain models were established containing the actual engine as-reflected in a series of selected operating points. We built an accurate gain-scheduling robust controller based on the estimation of performance degradation for a turbofan engine, with special focus on the problems discussed above. The main contributions of our work can be summarized as follows:

1) The on-board engine model can be updated online using the health parameters estimated by piecewise linearized Kalman filters; the improved on-board adaptive model provides accurate estimations of engine performance degradation.

2) The degradation term contained in the perturbation block in the engine uncertain models is eliminated. The perturbation radius of the engine uncertain models is reduced, the conservativeness of the designed robust controller is reduced, and the performance of the engine is improved on the whole.

3) Numerous operating points are selected under different working conditions and the degree of performance degradation in the full flight envelope of the engine. Robust controllers are then designed to guarantee stability and enhance the performance of uncertain models in the perturbation range. A gain-scheduling method which works based on scheduling parameters and engine performance degradation information is used to effectively control the engine in the full flight envelope.

The rest of this paper is organized as follows. Engine performance degradation is estimated in Section II. The robust controller design for uncertain models with health parameters is presented in Section III. Section IV presents the proposed robust gain-scheduled control design for uncertain models based on performance degradation. In Section V, simulation and verification results are given to evaluate the controller. Section VI concludes the paper and discusses relevant future research directions.

II. ESTIMATION OF ENGINE PERFORMANCE DEGRADATION

A. NONLINEAR ENGINE MODEL WITH HEALTH PARAMETERS

"Engine performance degradation" refers to the normal aging phenomenon characterized by natural wear, fatigue, fouling, and other factors after several cycles of operation.

Certain engine performance indicators slowly deviate from the rated state over time. The working efficiency of the turbine component, for example, slowly decreases as it services the engine for several cycles. The ability to convert high-temperature, high-pressure gas into mechanical energy is reduced and the linearized engine model at any one operating point changes accordingly.

Engine performance degradation is ultimately characterized by variations in operating efficiency and the gas flow of different rotor components, which are observable by changes in the efficiency coefficient and flow coefficient of the fan, compressor, main burner, and high- and low-pressure turbine components. These parameters characterizing engine performance degradation are often referred to as "health parameters".

Based on the component method, the nonlinear model of the engine with health parameters can be written as follows [41]

$$\dot{x}(t) = f(x(t), \quad u(t), h(t))$$
$$y(t) = g(x(t), \quad u(t), h(t)) \qquad (1)$$

where $u(t) \in R^m$ is the control input vector, $x(t) \in R^n$ is the state vector, $y(t) \in R^m$ is the output vector, $h(t) \in \mathcal{R}^l$ is the vector of health parameters, $f(\cdot)$ represents dynamics of the plant, and $g(\cdot)$ generates the plant outputs.

B. AUGMENTED STATE VARIABLE AEROENGINE MODEL

Considering the health parameter vector h as the control input of the engine, the small-perturbation method or the fitting method [42] can be used to linearize the engine nonlinear model at a healthy steady-state reference point as follows:

$$\begin{cases} \Delta\dot{x} = A_h\Delta x + B_h\Delta u_h + w \\ \Delta y = C_h\Delta x + D\Delta u_h + v \end{cases} \qquad (2)$$

where

$$A_h = A, \ B_h = (BL), \ C_h = C,$$
$$D_h = (DM), \ \Delta u_h = (\Delta u\Delta h)^T$$

where ω is system noise, υ is measuring noise, h represents the health parameters, and $\Delta h = h - h_0$.

An augmented linear state variable model which reflects the performance degradation of the engine can be written as

$$\begin{cases} \Delta\dot{x} = A\Delta x + B\Delta u + L\Delta h + w \\ \Delta y = C\Delta x + D\Delta u + M\Delta h + v \end{cases} \qquad (3)$$

where the matrices are obtained by

$$A = \frac{\partial f(.)}{\partial x(t)}|(x, u, h), \ B = \frac{\partial f(.)}{\partial u(t)}|(x, u, h),$$
$$L = \frac{\partial f(.)}{\partial h(t)}|(x, u, h)$$
$$C = \frac{\partial g(.)}{\partial x(t)}|(x, u, h), \ D = \frac{\partial g(.)}{\partial u(t)}|(x, u, h),$$

$$M = \frac{\partial g(.)}{\partial h(t)}|(x, u, h)$$

C. IMPROVED ON-BOARD ADAPTIVE MODEL

Health parameters are difficult or even impossible to measure. The parameters such as pressure, temperature, and rotational speed in each section of the engine can, however, be relatively easily measured; these are usually referred to as "measurement parameters". When the engine working environment does not change, changes in health parameters cause corresponding changes in the measured parameters. The two sets are related in an aerodynamic thermodynamic relationship. An optimal estimation filter can be designed to estimates the health parameters as per the measured parameters.

The engine performance degradation process is relatively slow, so it is reasonable to assume that $\Delta h = 0$. The health parameter can be further transformed into a set of state variables. Formula (3) can be rewritten as:

$$\begin{cases} \Delta\dot{x}_{new} = A_{new}\Delta x_{new} + B_{new}\Delta u + w \\ \Delta y = C_{new}\Delta x_{new} + D_{new}\Delta u + v \end{cases} \qquad (4)$$

where

$$A_{new} = \begin{pmatrix} A & L \\ 0 & 0 \end{pmatrix}, \quad B_{new} = \begin{pmatrix} B \\ 0 \end{pmatrix},$$
$$C_{new} = (CM), D_{new} = D, \quad \Delta x_{new} = \begin{pmatrix} \Delta x \\ \Delta h \end{pmatrix}.$$

1) TRADITIONAL ON-BOARD ADAPTIVE MODEL

The best estimate of the state variables in the form of Formula (4). The method most commonly used in engineering practice is the Kalman filter first proposed by the American-Hungarian mathematician Kalman in the late 1960s.

As mentioned above, Luppold *et al.* [34] first combined the engine on-board model with the Kalman filter to establish an on-board adaptive aeroengine model. The basic working principle is to correct the estimated state variables as per the error between the output data of the linear state variable model and the measured data of the actual engine, so as to correct the estimated state variables. The variance in the error between state variables and real state variables is minimized to achieve optimal filtering in the sense of minimum variance according to the estimated state variables for on-line correction of the on-board model under steady-state or quasi-steady state conditions. Thereby, effective online tracking for the real engine can be achieved.

2) IMPROVED ON-BOARD ADAPTIVE MODEL (IOBAM)

The steady-state reference value in the on-board adaptive model established by Kalman filter is usually obtained by interpolation method, but when there is a certain deviation of the steady-state reference value due to performance degradation for the engine in service, the estimation of the Kalman filter is biased. Thus, the on-board adaptive model loses its effectiveness in tracking the real engine.
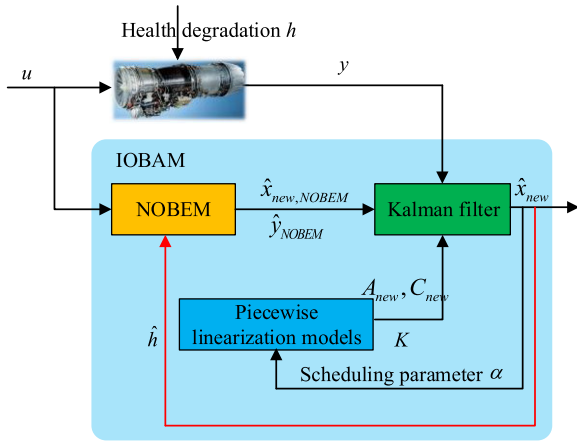
FIGURE 1. IOBAM structure.

FIGURE 2. Internal PLKF structure.

FIGURE 3. Output multiplicative perturbation configuration.

In this study, we developed an improved on-board adaptive model (IOBAM) by updating the nonlinear on-board engine model (NOBEM) using the health parameter vector estimated by the piecewise linearized Kalman filters (PLKF). The IOBAM mainly consists of two parts: the NOBEM based on performance degradation and the PLKF composed of piecewise linearization models and Kalman filters corresponding to their steady-state points. The basic working principle is to use the NOBEM output as the steady-state reference value of the PLKF, augment the health parameter in the form of Formula (4), perform online real-time estimation via the PLKF, and finally feed back to the NOBEM for online real-time updating. This technique allows for real-time tracking of real-world engines.

The main function of piecewise linearization models is to preserve the engine model parameters and their corresponding Kalman gain matrices under different working conditions by interpolation, and to schedule them based on the scheduling parameter α so that the Kalman filter adapts to different working states of the engine. In this study, the fan speed N_f was selected as the scheduling parameter α.

The structure of the proposed IOBAM is shown in Fig. 1. The Kalman estimation equation for Formula (4) is

$$\begin{cases} \Delta\dot{\hat{x}}_{new} = A_{new}\Delta\hat{x}_{new} + B_{new}\Delta u + K(\Delta y - \Delta\hat{y}) \\ \Delta\hat{y} = C_{new}\Delta x_{new} + D_{new}\Delta u \end{cases} \quad (5)$$

where K is the gain of Kalman filter satisfying $K = PC_{new}^T R^{-1}$; P is the solution to the Ricati equation $A_{new}P + PA_{new}^T + Q - PC_{new}^T R^{-1} C_{new} P = 0$.

The PLKF can be calculated using the healthy steady-state reference value $(x_{\text{NOBEM}}, u, y_{\text{NOBEM}}, h_{\text{NOBEM}})$ of the nonlinear on-board model instead of the healthy steady-state reference value (x_0, u_0, y_0, h_0) from Eq. (5) as follows:

$$\begin{cases} \dot{\hat{x}}_{new} = A_{new}\left(\hat{x}_{new} - x_{new,\text{NOBEM}}\right) + K(y - \hat{y}) \\ \hat{y} = C_{new}\left(\hat{x}_{new} - x_{new,\text{NOBEM}}\right) + y_{\text{NOBEM}} \end{cases} \quad (6)$$

The healthy steady-state reference value h_0, h_{NOBEM} is the health parameter value estimated by the Kalman filter at the
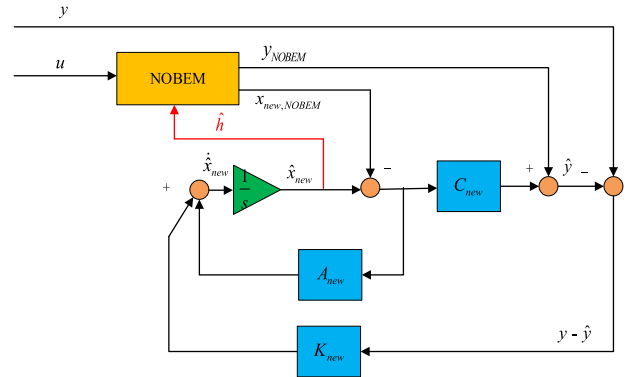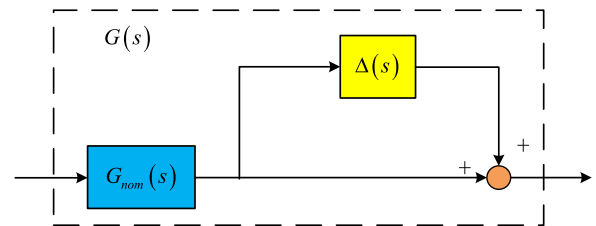
corresponding steady-state point under engine performance degradation conditions. The internal PLKF structure is shown in Fig. 2.

III. ROBUST CONTROLLER DESIGN FOR UNCERTAIN MODELS WITH HEALTH PARAMETERS
A. INTRODUCTION TO UNCERTAINTY
Uncertainty inevitably exists in any actual system [41] and may be characterized by external interference signals or model uncertainty. The external interference signals include input disturbance, output disturbance, and noise, among others. Model uncertainty expresses the difference or error between the actual plant and its mathematical representation.

Model uncertainty may have the following sources:

1) Inherent inaccuracies in the nonlinear model as- established;
2) Error in the linearization of the nonlinear model;
3) The unknown structure of the model (even at high frequencies), where uncertainty may exceed 100%;
4) Performance degradation of the actual plant due to abrasion and other factors causing error.

Uncertainty may adversely affect the stability and performance of a system.

B. UNCERTAIN MODELS WITH HEALTH PARAMETERS
The difference between the actual engine and its nominal model is expressed by a single perturbation block Δ. As shown in Fig. 3, we established engine uncertain models
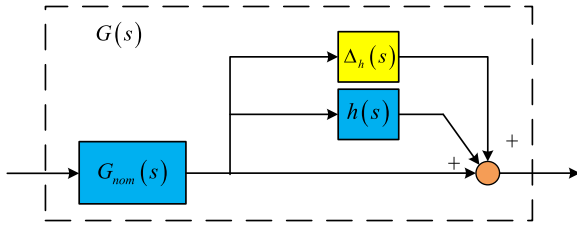
FIGURE 4. Perturbation configuration with performance degradation extracted.
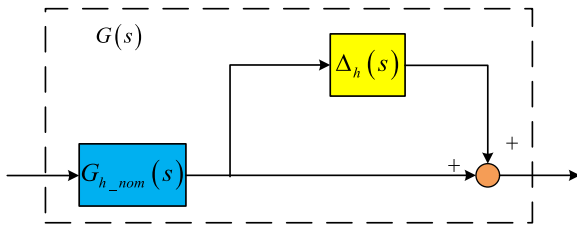

FIGURE 5. Perturbation configuration with performance degradation extracted.

with a perturbation block as follows:

$$
\begin{aligned}
\dot{x}(t) &= f(x(t), u(t)) \\
&= [I + \Delta_1] f_{nom}(x(t), u(t)) \\
y(t) &= g(x(t), u(t)) \\
&= [I + \Delta_2] g_{nom}(x(t), u(t))
\end{aligned} \tag{7}
$$

The above formula can be rewritten in the form

$$
G(s) = [I + \Delta(s)] G_{nom}(s) \tag{8}
$$

where $G(s)$ denotes uncertain models containing the model of the actual plant, $G_{nom}(s)$ is a nominal model, and $\Delta(s)$ is a perturbation block.

The perturbation block $\Delta(s)$ reflects the performance degradation (Fig. 4) and can be predicted by the measurement parameters. As shown in Fig. 5, we added the perturbation block with the health parameters to the nominal model and established new engine uncertain models as follows:

$$
\begin{aligned}
\dot{x}(t) &= f(x(t), u(t), h(t)) \\
&= [I + \Delta_{h1}] f_{nom}(x(t), u(t), h(t)) \\
y(t) &= g(x(t), u(t), h(t)) \\
&= [I + \Delta_{h2}] g_{nom}(x(t), u(t), h(t))
\end{aligned} \tag{9}
$$

The above formula can also be expressed in the form

$$
G(s) = [I + \Delta_h(s)] G_{h\_nom}(s) \tag{10}
$$

where $\Delta_h(s)$ denotes a perturbation block without engine performance degradation. $G_{h\_nom}(s)$ is the new nominal model established at the state of the engine performance degradation h, which satisfies the following:

$$
\begin{aligned}
G(s) &= [I + \Delta(s)] G_{nom}(s) \\
&= [I + \Delta_h(s) + h(s)] G_{nom}(s) \\
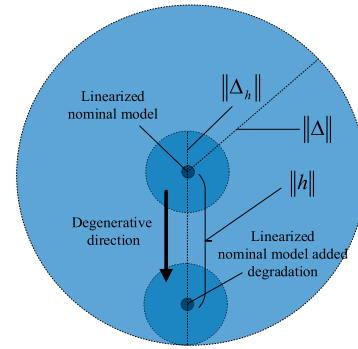&= [I + \Delta_h(s)] G_{h\_nom}(s)
\end{aligned}
$$

FIGURE 6. Uncertain model structure.

$$
G_{h\_nom}(s) = \left[\frac{h(s)}{I + \Delta_h(s)} + I \right] G_{nom}(s). \tag{11}
$$

In Fig. 6, the upper and lower small circled areas represent the linear uncertain models of the engine without degradation and with performance degradation h, respectively; the large circled area represents the linear uncertain models of the engine under general robust control. Engine degradation in the general robust controller is directly treated as an uncertainty in the engine model. Therefore, the radius of the uncertainty in the uncertain term must be large enough to contain the uncertain models of the engine under degradation, but this makes the perturbation radius of the uncertain model too large.

In this study, when the engine performance degrades by h, a new nominal model is established alongside engine uncertain models with the new nominal model as the center. By selecting a new nominal model in a different degraded state, we ensured that the perturbation radius of the uncertain models with minimum values cover all possible models of the engine.

As shown in Fig. 6, $\|\Delta_h\| = \|\Delta\| - \|h\| < \|\Delta\|$; by estimating engine performance degradation, the perturbation radius of the perturbation block in the engine uncertainty context can be reduced by $\|h\|$. The perturbation range of the uncertain model is reduced by:

$$
\frac{\|\Delta\|^2 - \|\Delta_h\|^2}{\|\Delta\|^2} * 100\% = \frac{\|h\|}{\|\Delta\|} \left(2 - \frac{\|h\|}{\|\Delta\|} \right) * 100\% \tag{12}
$$

C. $\mathcal{H}_\infty$ LOOP-SHAPING DESIGN

The $\mathcal{H}_\infty$ loop-shaping design [43], [44] for the multiple input multiple output system serves to solve a controller K to make the shaping of singular values for the transfer function satisfactory. This process and associated configuration are shown in Fig. 7. The controller K and plant G interconnection is driven by reference command r, input disturbance d_i, output disturbance d_o, and noise n. u represents the control signals and y the outputs to be controlled.

The following relationships hold:

$$
\begin{cases}
y = T_o(r - n) + GS_i d_i + S_o d_o \\
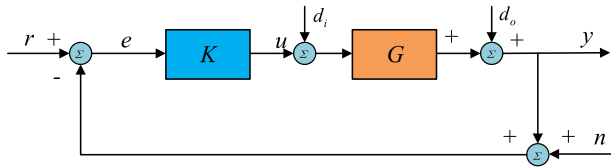e = S_o(r - d_o) + T_o n - GS_i d_i
\end{cases} \tag{13}
$$

FIGURE 7. Feedback configuration with disturbance and noise.

FIGURE 8. Nonlinear uncertain aeroengine model.

where $S_i = (I + KG)^{-1}$ expresses the transfer function from d_i to y, $S_o = (I + GK)^{-1}$ is the transfer function from d_o to y, and $T_o = GK(I + GK)^{-1}$ is the transfer function from n to y.

These relationships determine several closed-loop objectives:

1) For input disturbance attenuation, make $\bar{\sigma}(S_i(j\omega))$ small;
2) For output disturbance attenuation, make $\bar{\sigma}(S_o(j\omega))$ small;
3) For noise suppression, make $\bar{\sigma}(T_o(j\omega))$ small;
4) For good reference tracking, make $\bar{\sigma}(T_o(j\omega)) \approx \underline{\sigma}(T_o(j\omega)) \approx 1$.

The controller designed by the $\mathcal{H}_\infty$ loop-shaping design method has a high order which restricts its real-time performance and is difficult to achieve [45]. We used the absolute error approximation method [46] to appropriately degrade the designed robust controller to secure a reduced-order controller $K_r(s)$, i.e., to minimize

$$\| K(s) - K_r(s) \| . \tag{14}$$

IV. GAIN-SCHEDULED CONTROL DESIGN FOR UNCERTAIN MODELS WITH HEALTH PARAMETERS

The essence of gain-scheduling control is to design a set of linearized controllers and then combine them in a regular manner to be able to manipulate nonlinear systems. Gain-scheduling belongs to the category of adaptive control, but it differs from adaptive control in that it does not update feedback parameters through online identification, but through offline designed scheduling strategies.

First, the designer selects a set of parameter values which represent the range of the engine's dynamics. He or she then designs a linear time-invariant controller for each. Then, in between operating points, the controllers are interpolated for all frozen parameter values. Finally, a gain-scheduling controller for the nonlinear system is obtained.

The basic principle of robust gain-scheduling control with performance degradation is to select a series of operating points and obtain linearized models for the engine in the normal state and a state of certain performance degradation. Robust controllers are then designed with performance degradation isolated for the series of linearized models. The robust controllers can then be scheduled via scheduling and health parameters to control the system.
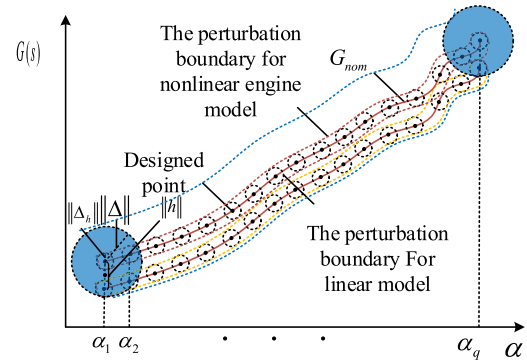
A. ROBUST CONTROLLER DESIGN FOR SELECTED OPERATING POINTS

We designed a gain-scheduling controller for the system reflected in Eq. (1) as discussed below [14], [15]. As shown in Fig. 8, we selected a family of operating points, $\alpha_i, i = 1, 2, \ldots, q$, which divide the flight envelope into q regions. At these operating points,

$$0 = f\left(x_{di}^p, u_{di}, h_{di}\right)$$
$$r_i = g\left(x_{di}^p, u_{di}, h_{di}\right) \tag{15}$$

where x_{di} is the ith selected operating point, u_{di} is the control input, and h_{di} represents the health parameters at x_{di}.

The linear model with health parameters at each selected operating point can be obtained by the small-perturbation method. The linear nominal models at the engine normal state and performance degradation h state can be obtained accordingly. Linear uncertain models at the normal state and performance degradation h state of each selected operating point for the engine are obtained once the perturbation block is added.

In Fig. 8, the upper and lower solid red lines respectively indicate the non-linear nominal model of the engine without degradation and with performance degradation h; the red and yellow dotted line enclosing areas respectively indicate the nonlinear uncertain models of the engine without degradation and with performance degradation h. The blue dotted area represents the nonlinear uncertain models of the engine in the general robust gain-scheduling controller design, which directly incorporates engine degradation as an uncertain term into the engine models.

Estimating the degradation of the engine and extracting it from the uncertainties of engine models can reduce the perturbation range of the engine nonlinear uncertain models. The perturbation range of the uncertain models is reduced by

$$\frac{\|\Delta_h\|}{\|\Delta\|} * 100\% = \left(1 - \frac{\|h\|}{\|\Delta\|}\right) * 100\%. \tag{16}$$

A series of robust controllers were designed in this study for the linear uncertain models at each selected operating point in the normal state of the engine and in a degraded state, respectively. The controllers were then obtained by linear
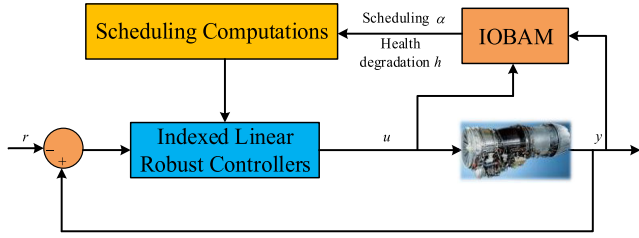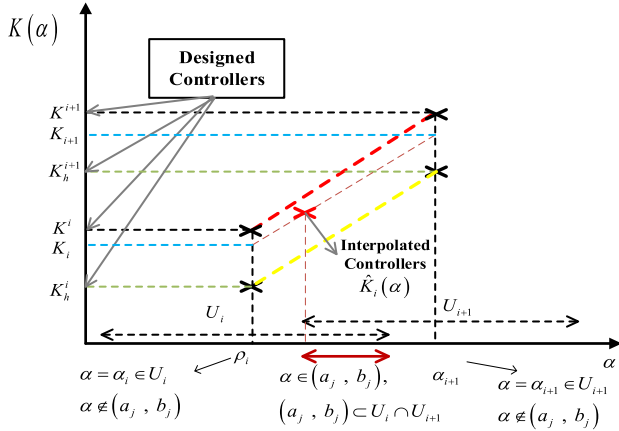
FIGURE 9. Gain-scheduling control system.

FIGURE 10. Controller interpolation schematics.

interpolation between the selected operating points to give the closed-loop system good robustness.

A structural diagram of the gain-scheduling control system is shown in Fig. 9. The parameter α represents the scheduling variable, which in this study is the fan speed of the engine. Another scheduling variable of the control system is a health parameter vector h that reflects engine performance degradation. The principle illustrated in Fig. 9 is to transmit the input parameter u and the output parameter y of the actual engine to the on-board adaptive model, perform scheduling calculation according to the scheduling parameter and the health degradation parameter h estimated by the model, and select the corresponding optimal robust controller for the engine to form a closed loop control system.

B. INTERPOLATION OF CONTROLLERS
A series of robust controllers were designed at the engine normal state and performance degradation h state at each selected operating point α_i in this study, which produced a set of controllers:

$$K^i := \begin{bmatrix} A_i^C & B_i^C \\ C_i^C & D_i^C \end{bmatrix}, \quad i = 1, 2, \ldots, q \tag{17}$$

$$K_{h\_base}^i := \begin{bmatrix} A_{i\text{-}h\text{-}base}^C & B_{i\text{-}h\text{-}base}^C \\ C_{i\text{-}h\text{-}base}^C & D_{i\text{-}h\text{-}base}^C \end{bmatrix}, \quad i = 1, 2, \ldots, q. \tag{18}$$

The controllers were interpolated based on the scheduling parameter α and health paramete h.

As shown in Fig. 10, based on the actual degree of degradation of the engine at the selected operating point α_i, the con-

troller K_i at the engine performance degradation h state can be obtained by linear interpolation using the controllers K^i and $K_{h\_base}^i$ at the engine normal state and performance degradation h_{base} state at the selected operating point α_i.

$$K_i = K^i + \frac{\|h\|}{\|h_{base}\|} \left(K_{h\_base}^i - K^i \right), \quad \forall \|h\| \in [0, \|h_{\max}\|] \tag{19}$$

As shown in Fig. 10, given the plant $\sum (\alpha)$, the stability interpolation method [47] generates controllers as follows:

$$K(\alpha(t), h(t))$$
$$:= \begin{cases} K_i, & \alpha \in U_i, \alpha \notin \cup_{i=1}^{q-1}[a_i, b_i], & i = 1, 2, \ldots q \\ \hat{K}_i(\alpha(t)), & \alpha \in [a_i, b_i], & i = 1, 2, \ldots q - 1 \end{cases} \tag{20}$$

where the controllers $\hat{K}_i(\alpha)$, $i = 1, 2, \ldots, q - 1$ can be linearly interpolated as

$$\hat{K}_i(\alpha(t)) = K_i + \frac{\alpha(t) - \alpha_i}{\alpha_{i+1} - \alpha_i}(K_{i+1} - K_i), \quad \forall \alpha \in [a_i, b_i] \tag{21}$$

V. TURBOFAN ENGINE EXAMPLE
The proposed robust gain-scheduling controller based on performance degradation was applied on a turbofan engine. We selected 45 operating points for the engine. The scheduling parameter α is the fan speed N_f. The performance degradation of the engine was indicated in this case by the health parameter vector h.

A. SIMULATION AT EACH OPERATING POINT
The linear nominal model with normalized and dimensionless dual inputs and dual outputs at each operating point can be written uniformly as:

$$\begin{cases} \Delta \dot{x} = A\Delta x + B\Delta u \\ \Delta y = C\Delta x + D\Delta u \end{cases} \tag{22}$$

where, $\Delta x = [\Delta_{PNF} \ \Delta_{PNC}]^T$ is the state variable, $\Delta y = [\Delta_{PNC} \ \Delta_{PT5}]^T$ is the output variable, $\Delta u = [\Delta_{PWF} \ \Delta_{PA8}]^T$ is the control variable, and $PWF = W_f/W_{f,d}$; $PA8 = A_8/A_{8d}$; $PNF = N_f/N_{f,d} PNC = N_c/N_{c,d}$; $PT5 = T_5/T_{5,d}$.

The subscript d represents engine parameters at the designed point. The uncertain models of the engine are written as:

$$G = (I_2 + \Delta W)G_{nom} \tag{23}$$

where

$$G_{nom}$$
$$= C(sI - A)^{-1}B + D$$
$$= \begin{bmatrix} \dfrac{0.3389\,s + 1.098}{s^2 + 11.02s + 20.9} & \dfrac{0.4046s^2 - 3.91s - 11.27}{s^2 + 11.02s + 20.9} \\ \dfrac{-0.2256\,s - 3.319}{s^2 + 11.02s + 20.9} & \dfrac{-0.0756s^2 - 8.382s - 26.55}{s^2 + 11.02s + 20.9} \end{bmatrix}$$
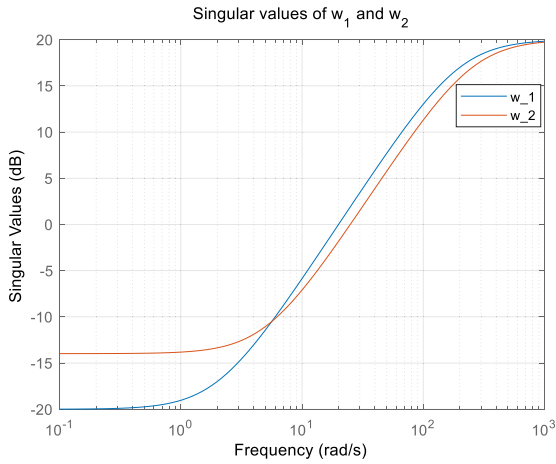
FIGURE 11. Singular value of weighting functions.

$$\Delta = \begin{bmatrix} \Delta_{ball1} & 0 \\ 0 & \Delta_{ball2} \end{bmatrix}, \quad |\Delta_{ball1}| < 1, |\Delta_{ball2}| < 1$$

and

$$W = \begin{bmatrix} w_1 & 0 \\ 0 & w_2 \end{bmatrix}$$

is a matrix which provides weighting functions for the perturbation block Δ.

1) BIG PERTURBATION BLOCK

Our focus in conducting this study was the range of low frequency when building the engine model, so the perturbation is greater in the high-frequency range. The singular values of w_1 and w_2 for the small perturbation block are shown in Fig. 11.

The final reduced-order controller can be calculated as

$$K = \begin{bmatrix} K_{11} & K_{12} \\ K_{21} & K_{22} \end{bmatrix} \tag{24}$$

where $K_{11}, K_{12}, K_{21}, K_{22}$ as shown at the bottom of the next page, Figure 12 shows the step responses of the uncertain closed-loop system. For all uncertain models, the largest settling times of the step response for the two outputs were 0.5 s and 0.8 s, respectively. The largest overshoots were 6% and 10%, respectively, and the steady-state error was 0.

2) SMALL PERTURBATION BLOCK

The perturbation block decreases in size after isolating the degradation term in the engine uncertainty models. The singular values of w_1 and w_2 for the small perturbation block are shown in Fig. 13.

The final reduced-order controller can be calculated as

$$K = \begin{bmatrix} K_{11} & K_{12} \\ K_{21} & K_{22} \end{bmatrix} \tag{25}$$

where $K_{11}, K_{12}, K_{21}, K_{22}$ as shown at the bottom of the next page, Figure 14 shows the step responses of the uncertain closed-loop system. The systems are stable in all uncertain models, which indicates that the designed controller has robust stability. The largest settling times of the step
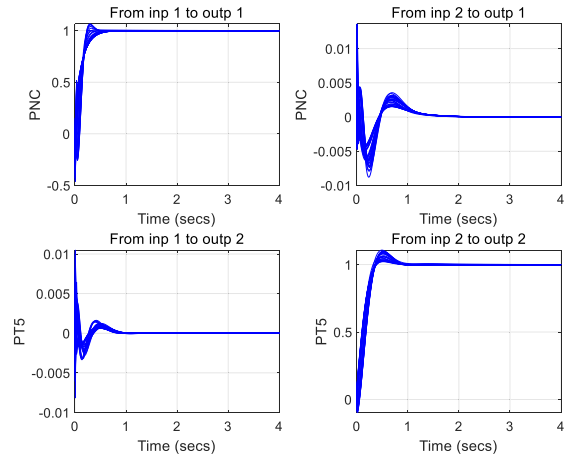

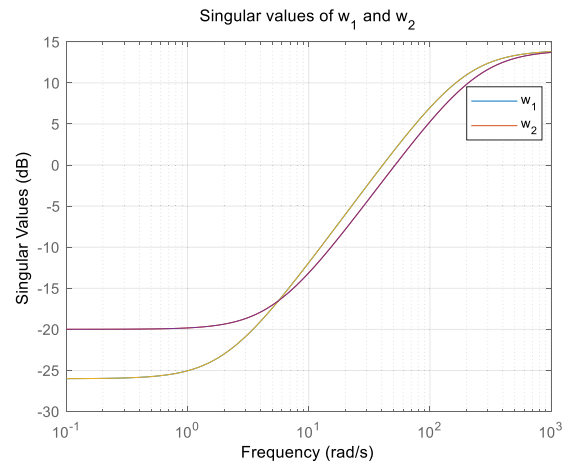**FIGURE 12.** Step responses of uncertain closed-loop system at 0 H and 0 Ma.

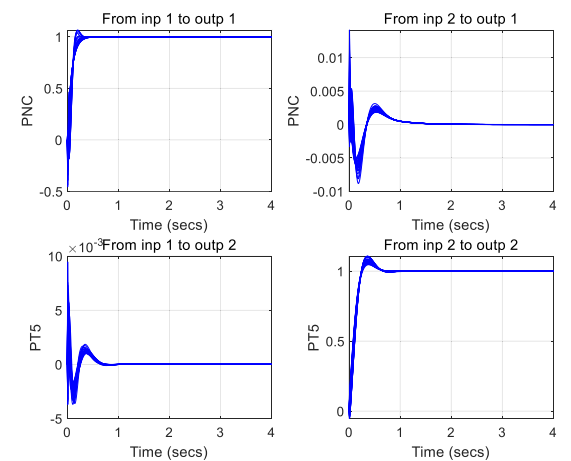**FIGURE 13.** Singular value of weighting functions.

FIGURE 14. Step responses of uncertain closed-loop system at 0 H and 0 Ma.

response for the two outputs in this case were 0.3 s and 0.5 s, respectively, the largest overshoots were 6% and 10%, respectively, and the steady-state error was 0. The mutual influence between the two channels was very small.
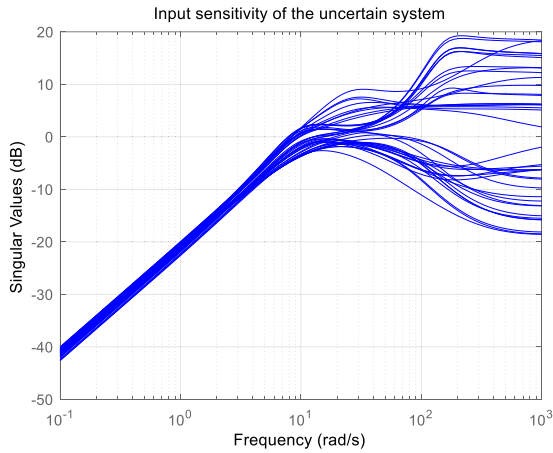
FIGURE 15. Singular values of S_i for uncertain system.

FIGURE 16. Singular values of S_o for uncertain system.

Under the same steady-state error and overshoot, the settling times of the two outputs of the closed-loop system with the small perturbation block decreased by 40% and 37.5%, respectively. The perturbation block is reduced after isolating the degradation term in the engine uncertainty models. The conservativeness of the proposed robust controller is thus reduced and the performance of the engine is greatly improved.

The singular values of S_i, S_o, and T_o for the uncertain system are shown in Fig. 15, Fig. 16, and Fig. 17, respectively. The singular values of S_i, S_o are very small in the low-frequency range, which suggests that the system can effectively suppress input disturbance and output disturbance. The singular value of T_o is very small in the high-frequency range, which indicates that the system can effectively suppress noise.

We next gave the nominal system a unit step input and added a step input disturbance with an amplitude of 0.2 at 3 s,
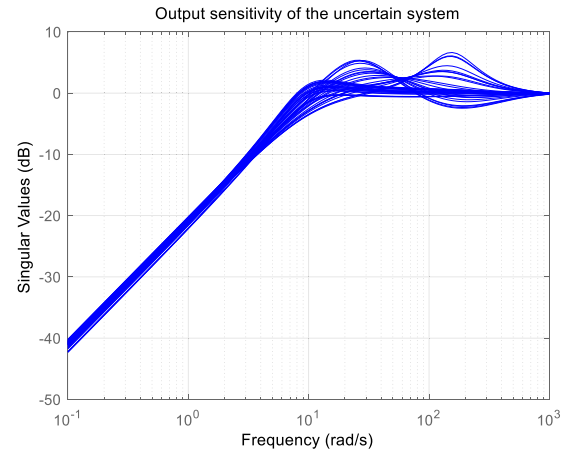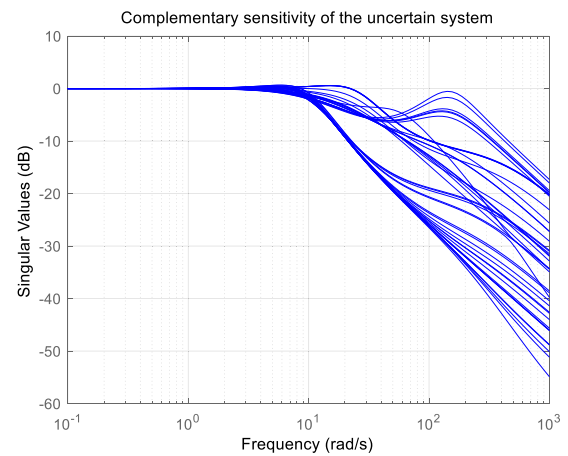

FIGURE 17. Singular values of T_o for uncertain system.

plus a step output disturbance with an amplitude of 0.2 at 5 s and a noise signal (Fig. 18) to the system.

$$
\begin{cases}
K_{11} = \dfrac{6.333 \times 10^4 s^3 + 7.025 \times 10^6 s^2 + 2.225 \times 10^7 s + 1.003 \times 10^{-5}}{s^4 + 4164 s^3 + 3.638 \times 10^5 s^2 + 7.035 \times 10^{-7} s + 1.886 \times 10^{-19}} \\[2mm]
K_{12} = \dfrac{3.389 \times 10^5 s^3 - 3.275 \times 10^6 s^2 - 9.449 \times 10^6 s - 6.358 \times 10^{-6}}{s^4 + 4164 s^3 + 3.638 \times 10^5 s^2 + 7.035 \times 10^{-7} s + 1.886 \times 10^{-19}} \\[2mm]
K_{21} = \dfrac{-1480 s^3 - 1.826 \times 10^5 s^2 - 2.89 \times 10^6 s + 2.233 \times 10^{-6}}{s^4 + 4164 s^3 + 3.638 \times 10^5 s^2 + 7.035 \times 10^{-7} s + 1.886 \times 10^{-19}} \\[2mm]
K_{22} = \dfrac{-7962 s^3 - 1.842 \times 10^5 s^2 - 9.752 \times 10^5 s - 3.967 \times 10^{-6}}{s^4 + 4164 s^3 + 3.638 \times 10^5 s^2 + 7.035 \times 10^{-7} s + 1.886 \times 10^{-19}}
\end{cases}
$$

$$
\begin{cases}
K_{11} = \dfrac{1.247 \times 10^5 s^3 + 1.383 \times 10^7 s^2 + 4.379 \times 10^7 s - 2.6 \times 10^{-5}}{s^4 + 4178 s^3 + 4.888 \times 10^5 s^2 - 1.165 \times 10^{-7} s - 9.815 \times 10^{-20}} \\[2mm]
K_{12} = \dfrac{6.672 \times 10^5 s^3 - 6.449 \times 10^6 s^2 - 1.86 \times 10^7 s + 9.152 \times 10^{-6}}{s^4 + 4178 s^3 + 488800 s^2 - 1.165 \times 10^{-7} s - 9.815 \times 10^{-20}} \\[2mm]
K_{21} = \dfrac{-2915 s^3 - 3.733 \times 10^5 s^2 - 5.947 \times 10^6 s + 2.489 \times 10^{-6}}{s^4 + 4178 s^3 + 488800 s^2 - 1.165 \times 10^{-7} s - 9.815 \times 10^{-20}} \\[2mm]
K_{22} = \dfrac{-1.567 \times 10^4 s^3 - 3.862 \times 10^5 s^2 - 2.05 \times 10^6 s - 2.492 \times 10^{-6}}{s^4 + 4178 s^3 + 488800 s^2 - 1.165 \times 10^{-7} s - 9.815 \times 10^{-20}}
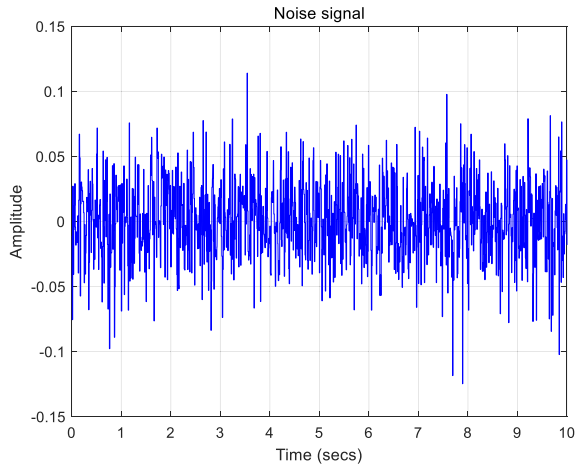\end{cases}
$$

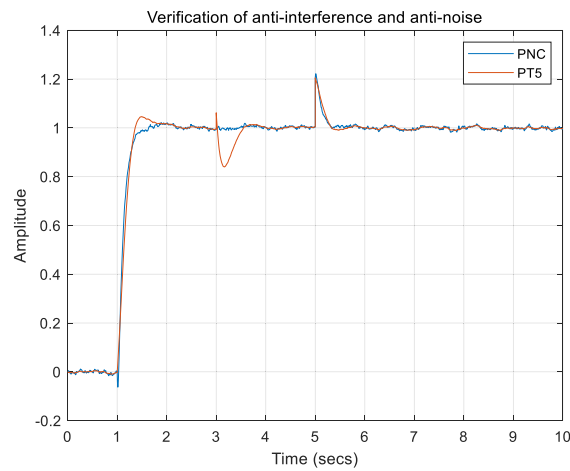**FIGURE 18.** Noise signal added on closed loop system.

FIGURE 19. Verification of anti-interference and anti-noise capabilities.

The simulation results reflecting the anti-interference and anti-noise performance of the nominal system are shown in Fig. 19. The influence of the input disturbance and the output disturbance on the system appears to be quickly offset within 0.5 s and 0.4 s, respectively, and the noise signal apparently has little influence on the system output. The system has good anti-interference and anti-noise capabilities.

Using the above method, we verified that the controllers designed at all operating points ensure closed-loop system stability, anti-interference capability, and anti-noise capability. For the sake of brevity and to prevent redundancy, only the average maximum settling time of small and large perturbation systems under the same steady-state error and overshoot at 10 typical operating points are provided here (Table 1). The "average maximum settling time" here refers to the average of the maximum settling times of the two output values of the dual-input and dual-output uncertain systems under the given step response. Under the same steady-state error and overshoot, the average settling time of the two outputs of the closed-loop system with the small perturbation block decreased by approximately 38%.

TABLE 1. Average maximum settling time of step response.

Fan Percentage Speed	Small Perturbation Block	Big Perturbation Block	Acceleration
50%	0.42s	0.68s	38.2%
55%	0.42s	0.69s	39.1
60%	0.41s	0.66s	37.9
65%	0.40s	0.66s	39.4
70%	0.41s	0.66s	37.9
75%	0.42s	0.68s	38.2
80%	0.40s	0.65s	38.5%
85%	0.39s	0.64s	39.1
90%	0.40s	0.64s	37.5
95%	0.41s	0.66s	37.9
Average Value	0.408s	0.662s	38.3%

B. SIMULATION OF ESTIMATED DEGRADATION PARAMETERS

The nominal state variable model with health parameters is

$$\begin{cases} \Delta \dot{x} = A \Delta x + B \Delta u + L \Delta h + w \\ \Delta y = C \Delta x + D \Delta u + M \Delta h + v \end{cases} \quad (26)$$

where $\Delta x = [\Delta_{PNF} \ \Delta_{PNC}]^T$ is a state variable, $\Delta y = [\Delta_{PNF} \ \Delta_{PNC} \ \Delta_{PP3} \ \Delta_{PT3} \ \Delta_{PP4} \ \Delta_{PP45} \ \Delta_{PT5} \ \Delta_{PP5} \ \Delta_{PP6} \ \Delta_{PT6} \ ]^T$ is an output variable, $\Delta u = [\Delta_{PWF} \ \Delta_{PA8}]^T$ is a control variable, and

$$\begin{aligned} \Delta h = [&\Delta \text{FAN\_ETA}, \ \Delta \text{HPC\_ETA}, \ \Delta \text{MainBurner\_ETA}, \\ &\Delta \text{HPT\_ETA}, \ \Delta \text{LPT\_ETA}, \ \Delta \text{FAN\_WA}, \\ &\Delta \text{HPC\_WA}, \ \Delta \text{MainBurner\_WA}, \ \Delta \text{HPT\_WG}, \\ &\Delta \text{LPT\_WH}]^T \end{aligned}$$

is a health parameter variable; w and v are system noise and measurement noise, respectively.

The zero-mean white noise with uncorrelated normal distribution and corresponding covariance matrices are Q and R; $Q = 0.005^2 I_{2 \times 2}$, $R = 0.001^2 I_{10 \times 10}$.

Let $\begin{aligned}\Delta h = [&-0.03, \ -0.03, \ -0.04, \ -0.03, \ -0.02, \\ &-0.03, \ -0.03, \ -0.04, \ -0.03, \ -0.05]^T\end{aligned}$.

The estimated health parameters are shown in Fig. 20, where the proposed model accurately and precisely estimates the degree of engine degradation.

C. SIMULATION FOR ROBUST GAIN-SCHEDULING CONTROLLER

By linear interpolation, we obtained a robust gain-scheduling controller based on performance degradation for an aero-engine in the flight envelope in this study. We selected four operating points in the flight envelope of the turbofan engine and used its nonlinear component-level model as the controlled object. The robust gain-scheduling controller was substituted for the control of engine. We made a wide range of speed steps at different operating points. We observed the step response effect through the obtained non-linear dynamic response data to verify the performance of the system.
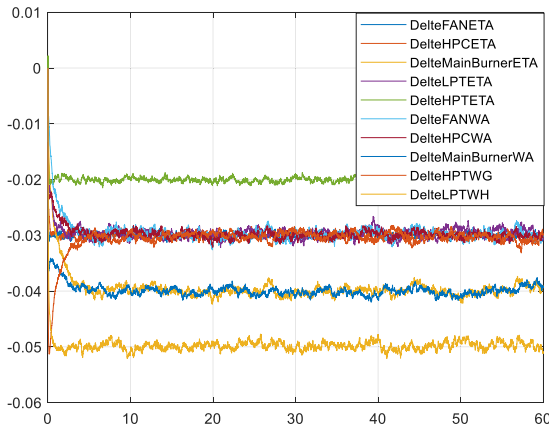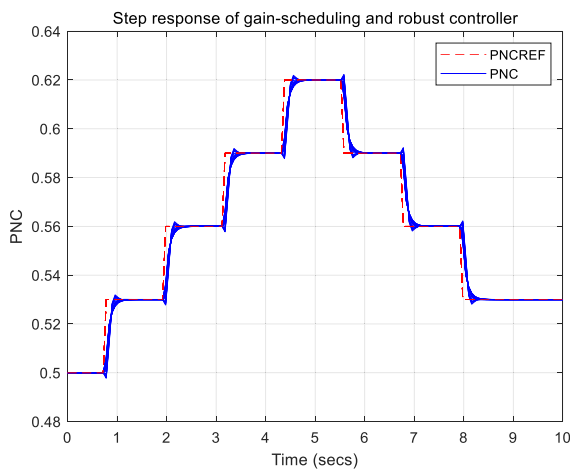
FIGURE 20. Estimated health parameters.

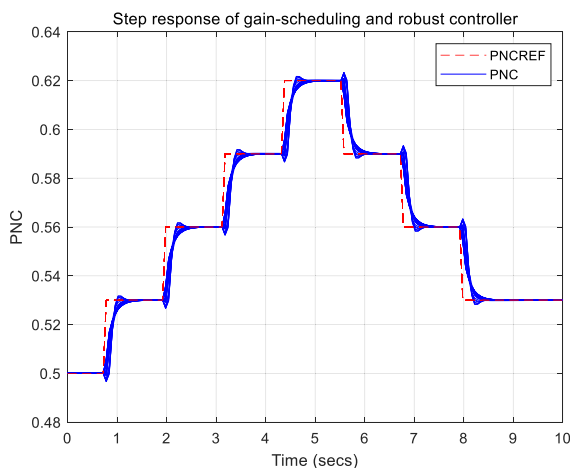**FIGURE 21.** Simulation for small perturbation system.

FIGURE 22. Simulation for large perturbation system.

The step responses of the small and large perturbation systems are shown in Fig. 21 and Fig. 22, respectively. The dashed red line represents the expected percentage speed of the compressor. The solid blue lines represent the actual percentage speed of the compressor of the uncertain system. As shown in Fig. 21, the designed controller gives the closed-loop system good tracking ability and the

robust gain-scheduling controller appears to guarantee stability in the entire parameter scheduling range under the variable parameter scheduling scheme; the system shows strong robustness.

By comparison against the results shown in Fig. 22, the response speed of the small perturbation system is better than that of the large perturbation system. The proposed controller greatly improves the performance of the system.

VI. CONCLUSION

A robust gain-scheduling control technique based on performance degradation for aeroengines was developed in this study. We first constructed an improved on-board adaptive aeroengine model to estimate engine performance degradation and eliminate the degradation term contained in the perturbation block of the engine uncertain models. Then, nonlinear uncertain models with engine health parameters were established and linear uncertain models of the engine were obtained by linearization at a series of operating points without degradation and with a certain degree of degradation, respectively. We also designed robust controllers at selected operating points without degradation and with a certain degree of degradation. The controllers of other non-selected operating points without degradation and with a certain degree of degradation were obtained by linear interpolation to establish the robust gain-scheduling controller.

Finally, we ran a series of simulations to find that the system has good robustness when equipped with the proposed controller. Compared with the traditional robust gain-scheduling controller, under the same overshoot, the proposed controller runs approximately 38% faster which markedly reduces its conservativeness.

A. FUTURE RECOMMENDATION

The controller design presented in this paper is based on the traditional gain-scheduling algorithm with health parameters introduced. Indeed, this is a relatively complicated design. The parameters are actually time-varying, so it is impossible to theoretically prove that the closed-loop system is globally stable and has desirable properties in the full flight envelope. It is typically impossible as well to assess a priori guarantee stability, robustness, and performance properties in gain-scheduling designs. Rather, any such properties are inferred from extensive computer simulations. These design steps are likewise highly complicated.

Robust gain-scheduling control based on LPV systems can, theoretically, ensure global stability and robustness while minimizing complexity. We plan to investigate this further in the near future.

REFERENCES

[1] M. Livshiz, D. J. Sanvido, and S. D. Stiles, "Nonlinear engine model for idle speed control," in *Proc. 33rd IEEE Conf. Decis. Control*, Dec. 1994, vol. 3, no. 2, pp. 2449–2451.

[2] Q. Z. Al-Hamdan and M. S. Y. Ebaid, "Modeling and simulation of a gas turbine engine for power generation," *J. Eng. Gas Turbines Power*, vol. 128, no. 2, pp. 302–311, Apr. 2006.

[3] X. Zhao, X. Wang, L. Ma, and G. Zong, "Fuzzy approximation based asymptotic tracking control for a class of uncertain switched nonlinear systems," *IEEE Trans. Fuzzy Syst.*, vol. 28, no. 4, pp. 632–644, Apr. 2020.

[4] H. Wang, P. X. Liu, J. Bao, X.-J. Xie, and S. Li, "Adaptive neural output-feedback decentralized control for large-scale nonlinear systems with stochastic disturbances," *IEEE Trans. Neural Netw. Learn. Syst.*, vol. 31, no. 3, pp. 972–983, Mar. 2020.

[5] H. Wang, P. X. Liu, X. Zhao, and X. Liu, "Adaptive fuzzy finite-time control of nonlinear systems with actuator faults," *IEEE Trans. Cybern.*, early access, May 8, 2019, doi: 10.1109/TCYB.2019.2902868.

[6] Y. Wang, B. Jiang, Z.-G. Wu, S. Xie, and Y. Peng, "Adaptive sliding mode fault-tolerant fuzzy tracking control with application to unmanned marine vehicles," *IEEE Trans. Syst., Man, Cybern. Syst.*, early access, Jan. 24, 2020, doi: 10.1109/TSMC.2020.2964808.

[7] Y. Wang, H. R. Karimi, H.-K. Lam, and H. Yan, "Fuzzy output tracking control and filtering for nonlinear discrete-time descriptor systems under unreliable communication links," *IEEE Trans. Cybern.*, early access, Jun. 17, 2019, doi: 10.1109/TCYB.2019.2920709.

[8] L. Ma, X. Huo, X. Zhao, and G. Zong, "Adaptive fuzzy tracking control for a class of uncertain switched nonlinear systems with multiple constraints: A small-gain approach," *Int. J. Fuzzy Syst.*, vol. 21, no. 8, pp. 2609–2624, Nov. 2019.

[9] Y. Yin, X. Zhao, and X. Zheng, "New stability and stabilization conditions of switched systems with mode-dependent average dwell time," *Circuits, Syst., Signal Process.*, vol. 36, no. 1, pp. 82–98, Jan. 2017.

[10] A. Kazemi, M. R. J. Motlagh, and A. H. Naghshbandy, "Application of a new multi-variable feedback linearization method for improvement of power systems transient stability," *Int. J. Elect. Power Energy Syst.*, vol. 29, no. 4, pp. 322–328, May 2007.

[11] C. Yang, C. Song, Z. Wu, and C. Xie, "Application of output feedback sliding mode control to active flutter suppression of two-dimensional airfoil," *Sci. China Technol. Sci.*, vol. 53, no. 5, pp. 1338–1348, May 2010.

[12] A. N. D. Lopes, V. J. S. Leite, L. F. P. Silva, and K. Guelton, "Anti-windup TS fuzzy PI-like control for discrete-time nonlinear systems with saturated actuators," *Int. J. Fuzzy Syst.*, vol. 22, no. 1, pp. 46–61, Feb. 2020.

[13] W. J. Rugh, "Analytical framework for gain scheduling," *IEEE Control Syst. Mag.*, vol. 11, no. 1, pp. 79–84, Jan. 1991.

[14] W. J. Rugh, and J. S. Shamma, "Research on gain scheduling," *Automatica*, vol. 36, no. 10, pp. 1401–1425, Oct. 2000.

[15] D. J. Leith and W. E. Leithead, "Survey of gain-scheduling analysis and design," *Int. J. Control*, vol. 73, no. 11, pp. 1001–1025, Jan. 2000.

[16] H. Kakigano, Y. Miura, and T. Ise, "Distribution voltage control for DC microgrids using fuzzy control and gain-scheduling technique," *IEEE Trans. Power Electron.*, vol. 28, no. 5, pp. 2246–2258, May 2013.

[17] D. Huang, J.-X. Xu, and V. Venkataramanan, "High performance tracking of piezoelectric positioning stage using current-cycle iterative learning control with gain scheduling," *IEEE Trans. Ind. Electron.*, vol. 61, no. 2, pp. 1085–1098, Feb. 2014.

[18] M. Sato and D. Peaucelle, "Gain-scheduled output-feedback controllers using inexact scheduling parameters for continuous-time LPV systems," *Automatica*, vol. 49, no. 4, pp. 1019–1025, Apr. 2013.

[19] M. R. Sathya and M. M. T. Ansari, "Load frequency control using bat inspired algorithm based dual mode gain scheduling of PI controllers for interconnected power system," *Int. J. Elect. Power Energy Syst.*, vol. 64, pp. 365–374, Jan. 2015.

[20] E. Kiyak, A. Kahvecioglu, and F. Caliskan, "Aircraft sensor and actuator fault detection, isolation, and accommodation," *J. Aerosp. Eng.*, vol. 24, no. 1, pp. 46–58, Jan. 2011.

[21] Y. Jung and D. H. Shim, "Development and application of controller for transition flight of tail-sitter UAV," *J. Intell. Robot. Syst., Theory Appl.*, vol. 65, nos. 1–4, pp. 137–152, Jan. 2012.

[22] M. Yasar and A. Ray, "Hierarchical control of aircraft propulsion systems: Discrete event supervisor approach," *Control Eng. Pract.*, vol. 15, no. 2, pp. 149–162, Feb. 2007.

[23] A. Rodriguez-Martinez, R. Garduno-Ramirez, and L. G. Vela-Valdes, "PI fuzzy gain-scheduling speed control at startup of a gas-turbine power plant," *IEEE Trans. Energy Convers.*, vol. 26, no. 1, pp. 310–317, Mar. 2011.

[24] W. Gilbert, D. Henrion, J. Bernussou, and D. Boyer, "Polynomial LPV synthesis applied to turbofan engines," *Control Eng. Pract.*, vol. 18, no. 9, pp. 1077–1083, Sep. 2010.

[25] I. Yazar, E. Kiyak, F. Caliskan, and T. H. Karakoc, "Simulation-based dynamic model and speed controller design of a small-scale turbo-jet engine," *Aircr. Eng. Aerosp. Technol.*, vol. 90, no. 2, pp. 351–358, Mar. 2018.

[26] S. Balamurugan, N. Janarthanan, and K. R. M. V. Chandrakala, "Small and large signal modeling of heavy duty gas turbine plant for load frequency control," *Int. J. Elect. Power Energy Syst.*, vol. 79, pp. 84–88, Jul. 2016.

[27] M. Pakmehr, N. Fitzgerald, E. M. Feron, J. S. Shamma, and A. Behbahani, "Gain scheduled control of gas turbine engines: Stability and verification," *J. Eng. Gas Turbines Power*, vol. 136, no. 3, pp. 1–15, Mar. 2014.

[28] K. Peng, D. Fan, F. Yang, L. Gou, and W. Lv, "A frequency domain decoupling method and multivariable controller design for turbofan engines," *IEEE Access*, vol. 5, pp. 27757–27766, 2017.

[29] G. Wolodkin, G. J. Balas, and W. L. Garrard, "Application of parameter-dependent robust control synthesis to turbofan engines," *J. Guid., Control, Dyn.*, vol. 22, no. 6, pp. 833–838, Nov. 1999.

[30] N. Aouf, D. G. Bates, I. Postlethwaite, and B. Boulet, "Scheduling schemes for an integrated flight and propulsion control system," *Control Eng. Pract.*, vol. 10, no. 7, pp. 685–696, Jul. 2002.

[31] D. K. Frederick, S. Garg, and S. Adibhatla, "Turbofan engine control design using robust multivariable control technologies," *IEEE Trans. Control Syst. Technol.*, vol. 8, no. 6, pp. 961–970, Nov. 2000.

[32] P. Apkarian and R. J. Adams, "Advanced gain-scheduling techniques for uncertain systems," *IEEE Trans. Control Syst. Technol.*, vol. 6, no. 1, pp. 21–32, Jan. 1998.

[33] Z. Liu, L. Gou, D. Fan, and Z. Zhou, "Design of gain-scheduling robust controller for aircraft engine," in *Proc. Chin. Control Conf. (CCC)*, Jul. 2019, pp. 870–875.

[34] R. Luppold, J. Roman, G. Gallops, and L. Kerr, "Estimating in-flight engine performance variations using Kalman filter concepts," in *Proc. 25th Joint Propuls. Conf.*, Monterey, CA, USA, Jul. 1989, pp. 10–13.

[35] X. Wei and G. Yingqing, "Aircraft engine sensor fault diagnostics based on estimation of Engine's health degradation," *Chin. J. Aeronaut.*, vol. 22, no. 1, pp. 18–21, Feb. 2009.

[36] X. Liu, N. Xue, and Y. Yuan, "Aircraft engine sensor fault diagnostics using an on-line OBEM update method," *PLoS ONE*, vol. 12, no. 2, 2017, Art. no. e0171037.

[37] F. Lu, Y. Chen, J. Huang, D. Zhang, and N. Liu, "An integrated nonlinear model-based approach to gas turbine engine sensor fault diagnostics," *Proc. Inst. Mech. Eng., G, J. Aerosp. Eng.*, vol. 228, no. 11, pp. 2007–2021, Sep. 2014.

[38] T. Kobayashi and D. L. Simon, "Integration of on-line and off-line diagnostic algorithms for aircraft engine health management," *J. Eng. Gas Turbines Power*, vol. 129, no. 4, pp. 986–993, Oct. 2007.

[39] X. Liu, Y. Yuan, J. Shi, and L. Zhao, "Adaptive modeling of aircraft engine performance degradation model based on the equilibrium manifold and expansion form," *Proc. Inst. Mech. Eng., G, J. Aerosp. Eng.*, vol. 228, no. 8, pp. 1246–1272, Jun. 2014.

[40] J. Lu, Y.-Q. Guo, and S.-G. Zhang, "Aeroengine on-board adaptive model based on improved hybrid Kalman filter," *J. Aerosp. Power*, vol. 26, no. 11, pp. 2593–2600, Nov. 2011.

[41] Q. Hu, and L. Xu, "Multi-objective compatible control algorithm for a class of uncertain model problem," *J. Tongji Univ.*, vol. 36, no. 4, pp. 525–529, Apr. 2008.

[42] L. Gou, X. Zeng, Z. Wang, G. Han, C. Lin, and X. Cheng, "A linearization model of turbofan engine for intelligent analysis towards industrial Internet of Things," *IEEE Access*, vol. 7, pp. 145313–145323, Oct. 2019.

[43] M. Osinuga, S. Patra, and A. Lanzon, "Incorporating smoothness into weight optimization for $\mathcal{H}_\infty$ loop-shaping design," in *Proc. 18th Medit. Conf. Control Automat. (MED)*, Jun. 2010, pp. 856–861.

[44] N. Ban and H. Ogawa, "A servo control system using the loop shaping design procedure," *World Acad. Sci., Eng. Technol.*, vol. 36, pp. 150–153, Dec. 2009.

[45] S. Gugercin and A. C. Antoulas, "A survey of model reduction by balanced truncation and some new results," *Int. J. Control*, vol. 77, no. 8, pp. 748–766, May 2004.

[46] D.-W. Gu, P. H. Petkov, and M. M. Konstantinov, "Lower-order controllers," in *Robust Control Design With MATLAB* (Advanced Textbooks in Control and Signal Processing). 2013, pp. 73–91.

[47] D. J. Stilwell and W. J. Rugh, "Stability preserving interpolation methods for the synthesis of gain scheduled controllers," *Automatica*, vol. 36, no. 5, pp. 665–671, May 2000.

LINFENG GOU received the Ph.D. degree from Northwestern Polytechnical University, in 2010. He is currently an Associate Professor of power control engineering with Northwestern Polytechnical University and the Vice President with the Power and Energy College. He has participated in many national key projects. His main research interests include fault diagnosis and fault tolerant control of aero-engine control systems.

DING FAN received the M.S. degree from Northwestern Polytechnical University, in 1984. He is currently a Professor of power control engineering with Northwestern Polytechnical University. His main research interest includes aircraft power control.

ZHIDAN LIU received the B.S. degree from the School of Power and Energy, Northwestern Polytechnical University, Xi'an, China, where he is currently pursuing the Ph.D. degree. His research interests include aero-engine control and fault diagnosis.

HUA ZHENG received the Ph.D. degree from Northwestern Polytechnical University, in 2011. He is currently an Associate Professor of power control engineering with Northwestern Polytechnical University. His main research interests include signal processing, modern measurement, and control technology.

● ● ●